ISSN 1674-1056
http://cpb.iphy.ac.cn
http://iopscience.iop.org/cpb
中国物理 B
Chinese Physics
中国物理 Chinese Physics B

Ultraviolet irradiation dosimeter based on persistent photoconductivity effect of ZnO

Chao-Jun Wang(王朝骏), Xun Yang(杨珣), Jin-Hao Zang(臧金浩), Yan-Cheng Chen(陈彦成), Chao-Nan Lin(林超男), Zhong-Xia Liu(刘忠侠), Chong-Xin Shan(单崇新)

Citation: Chin. Phys. B . 2020, 29(5): 058504 . **doi:** 10.1088/1674-1056/ab8891
Journal homepage: http://cpb.iphy.ac.cn; http://iopscience.iop.org/cpb

What follows is a list of articles you may be interested in

Thickness-modulated in-plane Bi_2O_2Se homojunctions for ultrafast high-performance photodetectors

Cheng-Yun Hong(洪成允), Gang-Feng Huang(黄刚锋), Wen-Wen Yao(要文文), Jia-Jun Deng(邓加军), Xiao-Long Liu(刘小龙)
Chin. Phys. B . 2019, 28(12): 128502 . **doi:** 10.1088/1674-1056/ab4e87

Enhanced performance of AlGaN-based ultraviolet light-emitting diodes with linearly graded AlGaN inserting layer in electron blocking layer

Guang Li(李光), Lin-Yuan Wang(王林媛), Wei-Dong Song(宋伟东), Jian Jiang(姜健), Xing-Jun Luo(罗幸君), Jia-Qi Guo(郭佳琦), Long-Fei He(贺龙飞), Kang Zhang(张康), Qi-Bao Wu(吴启保), Shu-Ti Li(李述体)
Chin. Phys. B . 2019, 28(5): 058502 . **doi:** 10.1088/1674-1056/28/5/058502

Metal halide perovskite photodetectors: Material featuresand device engineering

Ye Wang(王烨), Meng-Lei Gao(高孟磊), Jin-Liang Wu(吴金良), Xing-Wang Zhang(张兴旺)
Chin. Phys. B . 2019, 28(1): 018502 . **doi:** 10.1088/1674-1056/28/1/018502

Photon-counting chirped amplitude modulation lidar system using superconducting nanowire single-photon detector at 1550-nm wavelength

Hui Zhou(周慧), Yu-Hao He(何宇昊), Chao-Lin Lü(吕超林), Li-Xing You(尤立星), Zhao-Hui Li(李召辉), Guang Wu(吴光), Wei-Jun Zhang(张伟君), Lu Zhang(张露), Xiao-Yu Liu(刘晓宇), Xiao-Yan Yang(杨晓燕), Zhen Wang(王镇)
Chin. Phys. B . 2018, 27(1): 018501 . **doi:** 10.1088/1674-1056/27/1/018501

Zero-bias high-responsivity high-bandwidth top-illuminated germanium p–i–n photodetectors

Li Chong, Xue Chun-Lai, Liu Zhi, Cheng Bu-Wen, Li Chuan-Bo, Wang Qi-Ming
Chin. Phys. B . 2014, 23(3): 038506 . **doi:** 10.1088/1674-1056/23/3/038506

Ultraviolet irradiation dosimeter based on persistent photoconductivity effect of ZnO*

Chao-Jun Wang(王朝骏)[1,2], Xun Yang(杨珣)[1,2,†], Jin-Hao Zang(臧金浩)[1,2], Yan-Cheng Chen(陈彦成)[1,2], Chao-Nan Lin(林超男)[1,2], Zhong-Xia Liu(刘忠侠)[2], and Chong-Xin Shan(单崇新)[1,2,‡]

[1] *Henan Key Laboratory of Diamond Optoelectronic Materials and Devices, Key Laboratory of Materials Physics, Ministry of Education, School of Physics and Microelectronics, Zhengzhou University, Zhengzhou* 450052, *China*

[2] *Key Laboratory of Materials Physics, Ministry of Education, School of Physics and Microelectronics, Zhengzhou University, Zhengzhou* 450052, *China*

(Received 20 February 2020; revised manuscript received 29 March 2020; accepted manuscript online 12 April 2020)

It is essential to determine the accumulative ultraviolet (UV) irradiation over a period of time in some cases, such as monitoring UV irradiation to the skin, solar disinfection of water, photoresist exposure, etc. UV colorimetric dosimeters, which use dyes' color change to monitor the amount of UV exposure, have been widely studied. However, the exposure data of these UV colorimetric dosimeters can hardly be converted to digital signals, limiting their applications. In this paper, a UV dosimeter has been proposed and demonstrated based on the persistent photoconductivity (PPC) in zinc oxide microwires (ZnO MWs). The PPC effect usually results in high photoconductivity gain but low response speed, which has been regarded as a disadvantage for photodetectors. However, in this work, the unique characteristics of the PPC effect have been utilized to monitoring the accumulative exposure. We demonstrate that the photocurrent in the ZnO MWs depends on the accumulative UV exposure due to the PPC effect, thus the photocurrent can be utilized to determine the UV accumulation. The dosimeter is immune to visible light and exhibits a photoconductive gain of 2654, and the relative error of the dosimeter is about 10%. This UV dosimeter with electrical output is reusable and convenient to integrate with other electronic devices and may also open a new application area for the PPC effect.

Keywords: dosimetry, persistent photoconductivity, photodetectors, ultraviolet

PACS: 85.60.Gz, 42.79.Pw, 61.72.uj **DOI:** 10.1088/1674-1056/ab8891

1. Introduction

Ultraviolet (UV) irradiation can lead to serious skin diseases, and can also be applied in disinfection of water, photoresist exposure, and living cell inspection. In these cases, it is critically important to measure the amount of accumulative UV irradiation dose.[1–3] Currently, UV dosimeters based on color-responsive materials have been utilized to monitor the UV irradiation level, which are usually inaccurate and need a camera with complicated circuits to convert the exposure data to digital signals.[4,5] While traditional photodetectors that convert light to electrical signals are usually designed to measure the light intensity.[6–10] For practical applications, reusable dosimeters with electrical outputs are desperately desired. However, none such report can be found yet.

Persistent photoconductivity (PPC) effect has been widely observed in low-dimensional semiconductor materials, such as graphene, ZnO, SnO_2, InAs, *et al.*, in which the photogenerated carriers are gradually accumulated under the illumination light and can persist for a long period of time even after the exciting light is turned off.[10–16] Photodetectors based on the PPC effect usually demonstrate unique properties of high gain and high sensitivity but low response speed, which is regarded as a disadvantage for photodetectors. Wide bandgap semiconductor ZnO (3.37 eV) has been widely applied in UV photodetectors.[16–31] Meanwhile, the PPC effect has been reported in ZnO microwires (MW) photodetectors due to the surface oxygen absorption/desorption related processes.[32]

In this paper, the unique characteristics of the PPC effect are utilized to monitor the accumulative exposure. We demonstrate that the photocurrent of the ZnO MW is determined by the accumulative UV exposure because of the PPC effect, which can be attributed to the oxygen-related hole trap states at the ZnO MW surface. As a result, the UV accumulation over a period of time can be determined by comparing the photocurrent with previously measured photocurrent-UV exposure data as a reference. Then a reusable UV dosimeter with electrical output has been realized for the first time. The ZnO MW UV dosimeter is immune to visible light and exhibits a photoconductive gain of 2654 under low UV intensity (0.7 $\mu W/cm^2$) and a relative error of 10%. In this concept, reusable UV dosimeters with electrical output have been achieved, which is convenient to integrate with other functional electronic devices, providing a concept design in terms of PPC effect for potential applications.

*Project supported by the National Natural Science Foundation of China (Grant Nos. 61804136, U1604263, and U1804155) and China Postdoctoral Science Foundation (Grant Nos. 2018M630829 and 2019T120630).

†Corresponding author. E-mail: yangxun9013@163.com

‡Corresponding author. E-mail: cxshan@zzu.edu.cn

© 2020 Chinese Physical Society and IOP Publishing Ltd

2. Experimental details

The ZnO MWs used in this study were grown on silicon substrates in a horizontal alundum tube furnace via chemical vapor deposition (CVD) method. A mixture of ZnO and graphite powders with a definite weight ratio of 1 : 1 was used as the reactive source. During the growth process, a constant flow of argon (120 sccm) was introduced into the alundum tube as the protecting gas and the growth temperature was set at 1050 ℃. The structure and morphology properties of the as-grown ZnO MWs were investigated by using a Bruker D8 x-ray diffractometer (XRD) and a Hitachi S4800 field emission scanning electron microscope (SEM).

The schematic illustration of the ZnO MW dosimeter is shown in the inset of Fig. 1(a). To fabricate the ZnO MW dosimeter, an individual ZnO MW was picked out and placed onto a sapphire substrate. After that, two indium (In) particles were used to fix the two ends of the ZnO MW, also serving as the electrodes. The electrical characteristics of the single ZnO MW device were studied by a semiconductor characterization system (Keithley 4200-SCS) and the 365 nm light of a mercury lamp was used as the UV light source. The UV light intensity was measured by a commercial UV radiometer. The photoluminescence (PL) spectra of the ZnO MWs were studied employing the 325 nm line of a He–Cd laser as the excitation source. The response spectrum of the ZnO MW device was obtained in a photoresponse testing system with a Xe arc lamp as the light source. Without special instructions, all the measurements were carried out in air at room temperature.

3. Results and discussion

The XRD pattern of the ZnO MWs grown on Si substrate is shown in Fig. 1(a). All the peaks can be indexed to the diffraction from wurtzite ZnO.[33–35] The SEM image in Fig. 1(b) reveals the hexagonal structure of a single ZnO MW. The enlarged SEM image in the inset shows the rough surfaces of the ZnO MW, which may be related to the structural defects. The PL spectrum in Fig. 1(c) shows a near-band-edge emission peak at about 392 nm and a defect-related emission band at about 530 nm.[36,37] The strong defect-related emission confirms the existence of a larger number of defects on the ZnO MW surface, which have been reported to be responsible for the PPC effect in ZnO.[13,38–40]

An individual ZnO MW with a diameter of about 30.1 μm was picked out to fabricate the ZnO MW device, and the schematic diagram of the device is shown in the inset of Fig. 1(a). The distance between the two In electrodes is about 5 mm. Figure 2(a) presents some typical current–voltage (I–V) characteristics of the ZnO MW device in the dark or under UV illumination. The linear I–V curves indicate good ohmic contact between the ZnO MW and the In contacts. Under UV excitations, the current increases by an order of magnitude. The photoresponse characteristics were studied using time-resolved measurements with UV light switching on and off, as shown in Fig. 2(b). The current increases rapidly after the UV light is switched on and afterward at a slower rate. The current reaches a saturation value in about 2400 s. Then the current decays slowly after the UV light is turned off. The light switching cycles in Fig. 2(c) show good repeatability. Within the 6 cycles measured, the response speed and maximum/minimum current of each cycle are almost the same, indicating that the ZnO MW device has good reproducibility, which is essential for a reusable UV dosimeter.

The photoresponse spectrum of the ZnO MW device in the range of 200–800 nm is presented in Fig. 2(d). The onset of the photoresponse occurs at about 400 nm with the maximum at 376 nm. The photoresponse spectrum shows a blind response for visible light, which can avoid the use of any filters for the UV dosimeter. Figure 2(e) shows the measured photocurrent ($I_{ph} = I_{light} - I_{dark}$) as a function of the UV light intensity. As the UV light intensity increases from 0.7 μW/cm^2 to 371 μW/cm^2, the photocurrent increases gradually from 0.82 μA to 9.5 μA. Figure 2(f) exhibits the photoconductive gain derived from the same data in Fig. 2(e), according to $G = (I_{ph}/e)/(P/h\nu)$, where e is the elementary charge, P is the photon power absorbed by the ZnO MW, and $h\nu$ is the incident photon energy.[13] The photoconductive gain at 0.7 μW/cm^2 is 2654 and decreases gradually to about 58 as the light intensity increases to 371 μW/cm^2. The higher gain at lower light intensities and lower gain at higher light intensities ensure wide applicability of the UV dosimeter.

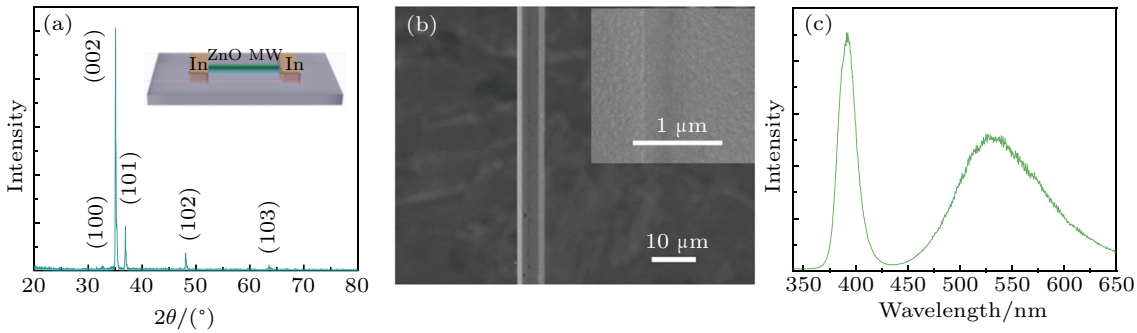


Fig. 1. Characterizations of the ZnO MWs. (a) XRD patterns of the ZnO MWs. The inset shows the schematic diagram of the ZnO MW based device. (b) SEM images of a single ZnO MW. The inset shows an enlarged SEM image of the surfaces. (c) PL spectrum of the ZnO MW.

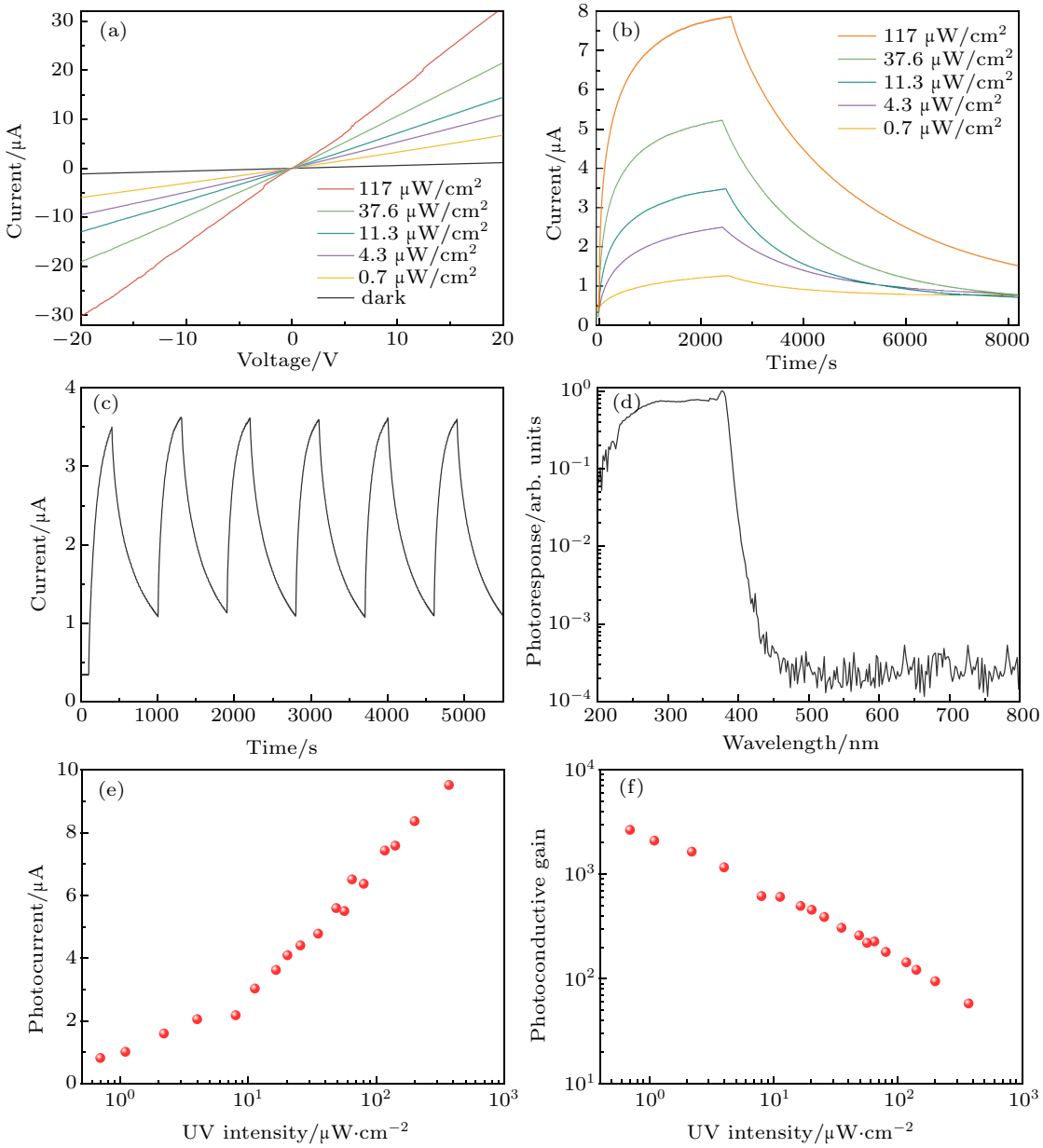


Fig. 2. Photoresponse characteristics of the ZnO MW device at 5 V bias. The 365 nm light of a mercury lamp is employed as the UV light source. (a) *I*–*V* curves as a function of light intensity. (b) Time-resolved photocurrent rise and decay with the illumination light switched on (at 0 s) and off (2400 s). (c) Repeatable response with UV light intensity of 37.6 μm/cm^2. (d) Response spectrum of the ZnO MW device in semilogarithmic coordinates. The dependence of photocurrent (e) and photoconductive gain (f) of the ZnO MW device on UV light intensity.

The high gain of the ZnO MW has been reported to result from the PPC effect related to desorption/re-adsorption of oxygen on the surface.[10,12] The photoresponse mechanism can be understood using the schematics shown in Figs. 3(a) and 3(b). Due to the high surface-to-volume ratio, there are a large amount of trapping states on the surface, which can affect the photoconductivity of the ZnO MW. In the dark, oxygen molecules are adsorbed on the surface of the ZnO MW, which can trap electrons from the conduction band, creating a low conductivity depletion layer near the surface (Fig. 3(a)). Under the illumination of photon with energy above the bandgap, electron–hole pairs are generated. The photogenerated holes may migrate to the surface and neutralize the negatively charged adsorbed oxygen ions. Then the neutral oxygen molecules are desorbed from the surface, and the unpaired electrons are left in the ZnO MW, contributing to the conductivity. Due to the separation, the lifetime of the electrons is greatly prolonged. Thus, the electrons can pass multiple times between the two electrodes, leading to a high photoconductive gain.[10,41,42] As the electrons previously trapped at the surface recombine with holes, the band bending lowers, as shown in Fig. 3(b). The probability that the electrons can reach the surface becomes higher. Some of the electrons will be trapped accompanying oxygen molecule re-adsorption. Therefore, the photocurrent saturates gradually, and the decrease of the photoconductive gain at higher UV intensities (Fig. 2(d)) is a manifestation of the saturation. To further confirm the photoresponse mechanism of the ZnO MWs,

we compare the photoresponse properties of the MWs in air and vacuum (2×10^{-4} Pa) at 5 V bias under the same UV light intensity, as presented in Fig. 3(c). The rise and decay processes can be well fitted with a double-exponential function. For the response curve in the air, the weight-averaged photocurrent rise and decay time constants of $\tau_{rise} = 39.2$ s and $\tau_{decay} = 261$ s can be deduced. The photocurrent decay time constant is more than 6 times larger than the rise time constant, which indicates that the oxygen re-adsorption process is a much slower process than the desorption one. While in the vacuum, the weight-averaged rise and decay time constants are $\tau_{rise} = 36.8$ s and $\tau_{decay} = 2526$ s, respectively. It is noted that the photocurrent in both cases rises with similar speed, while the decay is much faster for the MWs in the air than that in the vacuum. This is because oxygen molecules in the vacuum are continuously pumped away from the surface and the re-adsorption probability is very low.[13]

From the above discussion on the PPC photoresponse mechanism in the ZnO MWs, we know that the carriers generated by UV illumination are gradually accumulated in a period of time due to the slow desorption/re-sorption processes and long carrier lifetime. Therefore, the photoconductivity may be determined by the accumulative UV exposure. To study the relationship between the photocurrent and UV accumulation, we studied the photocurrent increase properties of a single ZnO MW device under 365 nm illumination. Figure 4(a) presents the transient photocurrent increase in UV light of different intensities (from 20 μW/cm^2 to 100 μW/cm^2). Figure 4(b) shows the relationship between the photocurrent and UV accumulation (calculated by integrating the light intensity over illumination time) obtained from the same data in Fig. 4(a). One can see that all the curves show similar UV accumulation at the same photocurrent. Figure 4(c) shows the plots of the mean UV accumulation and corresponding relative standard deviation (RSD) versus photocurrent. The RSD at small UV accumulation is about 26%, while it decreases to around 10% when the UV accumulation is larger than 150 mJ/cm^2. The relatively larger RSD at lower UV accumulation may result from the rapid photocurrent rise speed immediately after switching on the UV light, leading to large measurement errors of photocurrent and UV accumulation. While the relatively smaller RSD at larger UV accumulation indicates that the photocurrent would be the same under the same UV accumulation despite the UV light intensity, confirming the assumption that the photocurrent in the ZnO MWs depends on the accumulative UV exposure. Therefore, it is promising to determine the UV accumulation during a period of time using the photocurrent of the ZnO MWs.

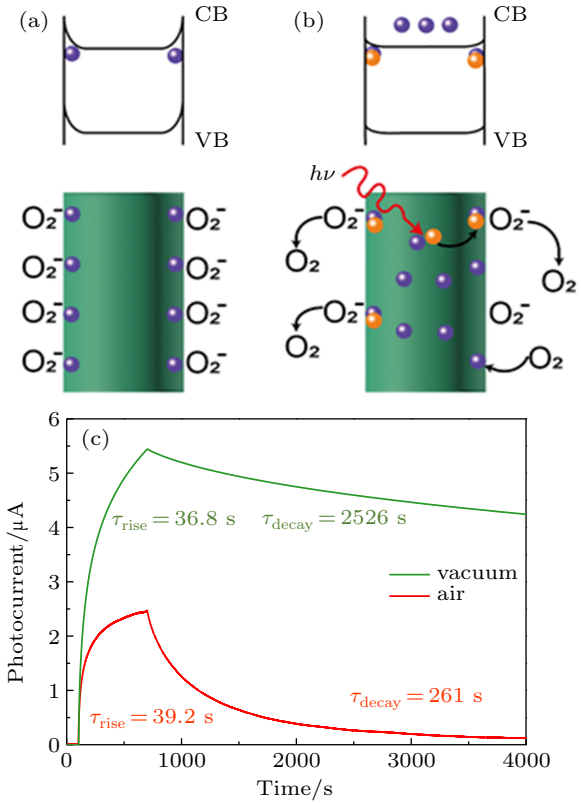


Fig. 3. Persistent photoconductivity in the ZnO MW device. (a), (b) Trapping and photoconduction mechanism in the ZnO MW. The top panel in (a) shows the schematic energy band diagram of the ZnO MW in the dark. CB and VB are the conduction and valence bands, respectively. The bottom panel shows oxygen molecules adsorbed on the ZnO MW surface that capture free electrons, resulting in a low-conductivity depletion layer near the surface. The top panel in (b) shows the schematic energy band diagram of the ZnO MW under UV illumination. Photogenerated holes migrate to the surface and recombine with the trapped electrons, releasing the absorbed oxygen molecules. The unpaired electrons in the MW contribute to the photoconductivity. (c) Time-resolved photocurrent rise and decay of the ZnO MW device in air and vacuum.

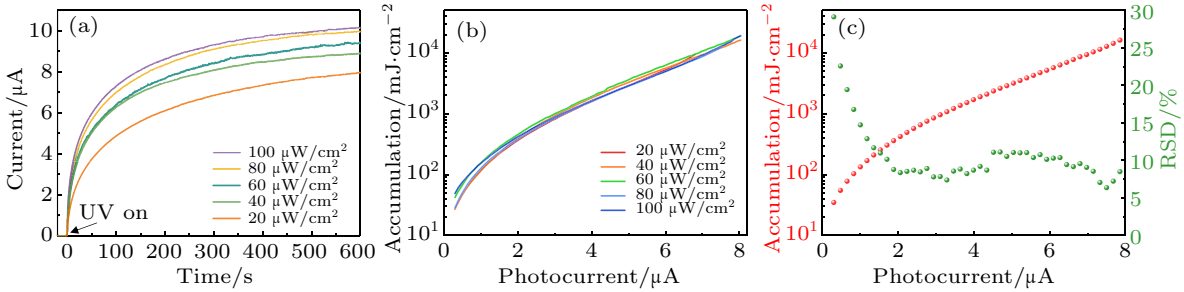


Fig. 4. Relationship between photocurrent and accumulative UV exposure of the ZnO MW device. (a) Time-resolved photocurrent increase under different UV light intensity of the ZnO MW device. (b) The relationships between photocurrent and UV accumulation, obtained from the same data in (a). (c) The mean UV accumulation and corresponding relative standard deviation versus photocurrent. All measurements were performed at 5 V bias.

Figure 5(a) shows the time-resolved photocurrent measurements of the same ZnO MW studied in Fig. 4. During the two tests (test-1 and test-2), the UV light density is changed intermittently. The relationship between the UV accumulation and photocurrent in the two tests is presented in Fig. 5(b), together with the plot of the mean UV accumulation versus photocurrent from Fig. 4(c) as a reference. Both the two UV accumulation versus photocurrent curves of test-1 and test-2 are in good agreement with the reference plot. Thus, the UV accumulation can be determined by comparing the photocurrent of the ZnO MW device with the reference plot. To estimate the accuracy of this method, we calculated the relative error between the actual UV accumulation and the deduced UV accumulation, as presented in Fig. 5(c). The relative error is larger than 10% at low UV accumulation and decreases to around or below 10% at UV accumulation larger than 100 mJ/cm^2. Therefore, the relative error of the ZnO MW UV dosimeter is about 10% when the UV accumulation is larger than 100 mJ/cm^2.

To investigate the immunity to visible light of the ZnO MW UV dosimeter, which is crucial for the future application of the UV dosimeter, another test with the presence of visible light has been carried out. Figure 6(a) shows the curve of UV accumulation versus photocurrent of the ZnO MW UV dosimeter measured with the presence of visible light, of which the spectrum is shown in the inset of Fig. 6(b). The UV accumulation–photocurrent relationship also agrees well with the reference plot. The relative error of the deduced UV is presented in Fig. 6(b), which is lower than 12% at UV accumulation larger than 100 mJ/cm^2, similar to the results of tests in the absence of visible light. Thus, the ZnO MW UV dosimeter is immune to visible light because the ZnO MW device response barely to visible light (Fig. 2(d)).

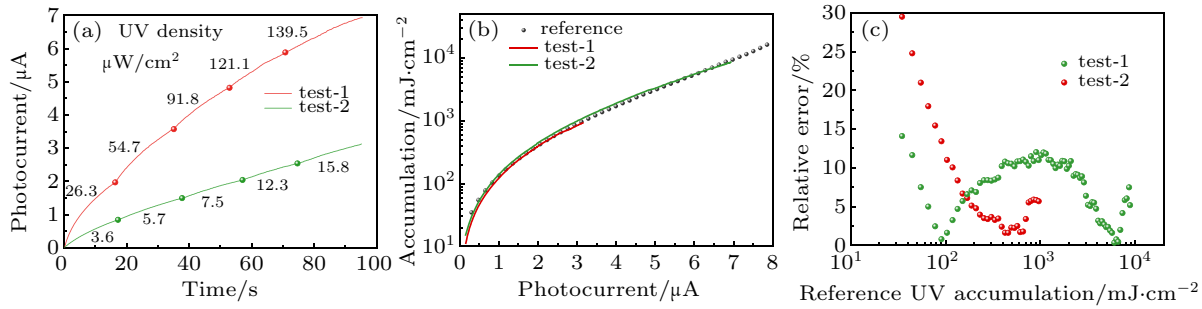


Fig. 5. Method for determining the UV accumulation using photocurrent. (a) Time-resolved photocurrent changes of the ZnO MW device when the UV light intensity changes intermittently. The two curves present two different test processes (test-1 and test-2). The UV light intensity of each period is denoted in the figure. (b) The relationship between photocurrent and UV accumulation in the two tests, compared with the reference plot from Fig. 4(c). (c) The relative error of the inferred UV accumulation for the two tests.

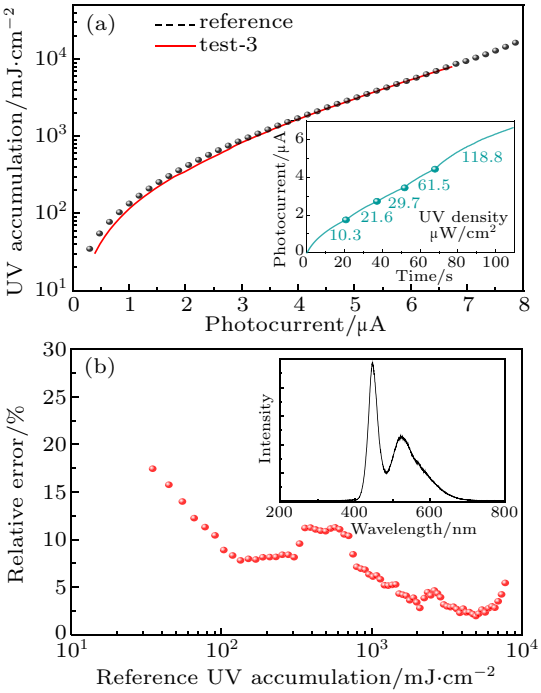


Fig. 6. The ZnO MW UV dosimeter response with the presence of visible light emitted from interior fluorescent lamps (37 μm/cm^2). (a) The relationship between photocurrent and UV accumulation compared with the reference plot. The inset shows the time-resolved photocurrent changes. (b) Relative error of the deduced UV accumulation.

4. Conclusion

In this paper, a UV dosimeter has been realized from ZnO MW based photodetectors based on the persistent photoconductivity effect. The accumulative UV exposure can be deduced by comparing the photocurrent of the ZnO MWs with the reference UV accumulation–photocurrent relationship. The relative error of the measured accumulative UV irradiation is around 10%. Moreover, this UV dosimeter is immune to visible light because of the wide bandgap of ZnO. The ZnO MW based UV dosimeter with electrical output signals could be more easily integrated with other electronic devices. Thus, the UV dosimeter opens up a cost-effective way to monitor the accumulative UV exposure, providing a concept design for further potential applications.

References

[1] Araki H, Kim J, Zhang S, Banks A, Crawford K E, Sheng X, Gutruf P, Shi Y, Pielak R M and Rogers J A 2017 *Adv. Funct. Mater.* **27** 1604465
[2] Humble M B 2010 *J. Photochem. Photobiol. B* **101** 142
[3] Chen Y C, Lu Y J, Liu Q, Lin C N, Guo J, Zang J H, Tian Y Z and Shan C X 2019 *J. Mater. Chem. C* **7** 2557
[4] Mills A, McFarlane M and Schneider S 2006 *Anal. Bioanal. Chem.* **386** 299

[5] Kim J, Salvatore G A, Araki H, Chiarelli A M, Xie Z, Banks A, Sheng X, Liu Y, Lee J W, Jang K I, Heo S Y, Cho K, Luo H, Zimmerman B, Kim J, Yan L, Feng X, Xu S, Fabiani M, Gratton G, Huang Y, Paik U and Rogers J A 2016 *Sci. Adv.* **2** e1600418

[6] Shan C X, Liu J S, Lu Y J, Li B H, Ling F C C and Shen D Z 2015 *Opt. Lett.* **40** 3041

[7] Li Y, Shi Z F, Lei L Z, Ma Z Z, Zhang F, Li S, Wu D, Xu T T, Li X J, Shan C X and Du G T 2018 *ACS Photon.* **5** 2524

[8] Yang X, Shan C X, Lu Y J, Xie X H, Li B H, Wang S P, Jiang M M and Shen D Z 2016 *Opt. Lett.* **41** 685

[9] Liu Y, Jiang M M, Zhang Z, Li B H, Zhao H, Shan C X and Shen D Z 2018 *Nanoscale* **10** 5678

[10] Kim T, Park S, Kang H K, Jeong K, Bae J, Song J and Cho M H 2018 *Appl. Surf. Sci.* **458** 964

[11] Liu S, Liao Q L, Zhang Z, Zhang X K, Lu S N, Zhou L X, Hong M Y, Kang Z and Zhang Y 2017 *Nano Res.* **10** 3476

[12] Liu K W, Sakurai M, Aono M and Shen D Z 2015 *Adv. Funct. Mater.* **25** 3157

[13] Soci C, Zhang A, Xiang B, Dayeh S A, Aplin D P R, Park J, Bao X Y, Lo Y H and Wang D 2007 *Nano Lett.* **7** 1003

[14] Tian Y, Guo C F, Zhang J and Liu Q 2015 *Phys. Chem. Chem. Phys.* **17** 851

[15] Biswas C, Güneş F, Loc D D, Lim S C, Jeong M S, Pribat D and Lee Y H 2011 *Nano Lett.* **11** 4682

[16] Lu L Z, Jiang X T, Peng H Q, Zeng D and Xie C S 2018 *RSC Adv.* **8** 16455

[17] Du J L, Liao Q L, Hong M Y, Liu B S, Zhang X K, Yu H H, Xiao J K, Gao L, Gao F F, Kang Z, Zhang Z and Zhang Y 2019 *Nano Energy* **58** 85

[18] Zhou C Q, Ai Q, Chen X, Gao X H, Liu K Y and Shen D Z 2019 *Chin. Phys. B* **28** 048503

[19] Liu K K, Li X M, Cheng S B, Zhou R, Liang Y C, Dong L, Shan C X, Zeng H B and Shen D Z 2018 *Nanoscale* **10** 7155

[20] Lu Y J, Shi Z F, Shan C X and Shen D Z 2017 *Chin. Phys. B* **26** 047703

[21] Lin P, Yan X Q, Zhang Z, Shen Y W, Zhao Y G, Bai Z M and Zhang Y 2013 *ACS Appl. Mater. Inter.* **5** 3671

[22] Yang X, Shan C X, Liu Q, Jiang M M, Lu Y J, Xie X H, Li B H and Shen D Z 2018 *ACS Photon.* **5** 1006

[23] Bao R R, Wang C F, Peng Z C, Ma C, Dong L and Pan C F 2017 *ACS Photon.* **4** 1344

[24] Zhang Z, Kang Z, Liao Q L, Zhang X M and Zhang Y 2017 *Chin. Phys. B* **26** 118102

[25] Shi Z F, Sun X G, Wu D, Xu T T, Zhuang S W, Tian Y T, Li X and Du G T 2016 *Nanoscale* **8** 10035

[26] Ni P N, Shan C X, Wang S P, Lu Y J, Li B H and Shen D Z 2015 *Appl. Phys. Lett.* **107** 231108

[27] Zang S P, Wang Y L, Li M Y, Su W, An M Q, Zhang X T and Liu Y C 2018 *Chin. Phys. B* **27** 018503

[28] Liu Z Y, Shen C L, Lou Q, Zhao W B, Wei J Y, Liu K K, Zang J H, Dong L and Shan C X 2020 *J. Lumin.* **221** 117111

[29] Madel M, Huber F, Mueller R, Amann B, Dickel M, Xie Y and Thonke K 2017 *J. Appl. Phys.* **121** 124301

[30] Gao T, Ji Y and Yang Y 2019 *Adv. Electron. Mater.* **5** 1900776

[31] Rana A K, Kumar M, Ban D, Wong C, Yi J and Kim J 2019 *Adv. Electron. Mater.* **5** 1900438

[32] Li H X, Zhang X H, Liu N S, Ding L W, Tao J Y, Wang S L, Su J, Li L Y and Gao Y H 2015 *Opt. Express* **23** 21204

[33] Chen A Q, Zhu H, Wu Y Y, Lou G L, Liang Y F, Li J Y, Chen Z Y, Ren Y H, Gui X C, Wang S P and Tang Z K 2017 *ACS Photon.* **4** 1286

[34] Zhang Q, Qi J J, Li X, Yi F, Wang Z Z and Zhang Y 2012 *Appl. Phys. Lett.* **101** 043119

[35] Yang X, Shan C X, Ni P N, Jiang M M, Chen A Q, Zhu H, Zang J H, Lu Y J and Shen D Z 2018 *Nanoscale* **10** 9602

[36] Shi Z F, Xu T T, Wu D, Zhang Y T, Zhang B L, Tian Y T, Li X and Du G T 2016 *Nanoscale* **8** 9997

[37] Chen A Q, Zhu H, Wu Y Y, Chen M M, Zhu Y, Gui X C and Tang Z K 2016 *Adv. Funct. Mater.* **26** 3696

[38] Hullavarad S, Hullavarad N, Look D and Claflin B 2009 *Nanoscale Res. Lett.* **4** 1421

[39] Laiho R, Poloskin D S, Stepanov Y P, Vlasenko M P, Vlasenko L S and Zakhvalinskii V S 2009 *J. Appl. Phys.* **106** 013712

[40] Liu P, She G W, Liao Z L, Wang Y, Wang Z Z, Shi W S, Zhang X H, Lee S T and Chen D M 2009 *Appl. Phys. Lett.* **94** 063120

[41] Katz O, Garber V, Meyler B, Bahir G and Salzman J 2001 *Appl. Phys. Lett.* **79** 1417

[42] Reparaz J S, Guell F, Wagner M R, Hoffmann A, Cornet A and Morante J R 2011 in *2011 Conference on Lasers and Electro-Optics Europe and* 12*th European Quantum Electronics Conference* (IEEE, Munich, Germany), p. 1